International Journal of Applied Mathematics

Volume 38 No. 1s, 2025

ISSN: 1311-1728 (printed version); ISSN: 1314-8060 (on-line version)

EFFECT OF DUFOUR ON UNSTEADY MHD CASSON FLUID FLOW OVER A VERTICAL SURFACE USING LAPLACE TRANSFORMATION

S.Dinesh[1], S.Lakshmi Priya[2*]

[1]Department of Mathematics and Statistics,

Faculty of Science and Humanities,

SRM Institute of Science and Technology,

Kattankulathur 603203, Chengalpattu, INDIA

mail : ds7870@srmist.edu.in

[2]Department of Mathematics and Statistics,

Faculty of Science and Humanities,

SRM Institute of Science and Technology,

Kattankulathur 603203, Chengalpattu, INDIA

Email : lakshmis3@srmist.edu.in

ABSTRACT

This paper presents an analytical investigation of unsteady magneto hydrodynamic (MHD) flow of a Casson fluid streaming along an exponentially infinite vertical surface, incorporating the Dufour effect. In this study, we extend the existing Laplace transform solution methodology to account for the flow model with Dufour effect. The dynamics are governed by coupled partial differential equations portraying the momentum, energy, and concentration fields. The Casson fluid behaviour, magnetic field effects, and chemical reaction parameter are incorporated into the governing equations, and a solution is obtained using the Laplace transform technique. The results illustrates the consequential leverage of the chemical reaction parameter on the velocity, temperature, and concentration profiles. And some variables like magnetic field M, Casson fluid parameter β, Grashof number Gr, Prandtl number Pr, Thermal radiation Rd and Schmidt number Sc are being analysed. The findings provide insights into optimizing industrial processes where Dufour effect and magnetic fields interact with non-Newtonian fluids. This study accords to a more comprehensive interpretation of the MHD flow of Casson fluids, with implications for heat and mass transfer applications.

Math Subject Classification:

76-10 Mathematical modeling or simulation for problems pertaining to fluid mechanics.

35G15 Boundary value problems for linear higher-order PDEs

34A34 Nonlinear ordinary differential equations and systems

Received: July 14, 2025

Volume 38 No. 1s, 2025

ISSN: 1311-1728 (printed version); ISSN: 1314-8060 (on-line version)

76D55 Flow control and optimization for incompressible viscous fluids

76E25 Stability and instability of magnetohydrodynamic and electrohydrodynamic flows

KEYWORDS: MHD, Dufour effect, Chemical reaction, Thermal radiation, Casson fluid

INTRODUCTION:

Casson fluid is a sort of non-Newtonian fluid that is used in many innovative ways in medicine and industry. This has led to a lot of research into it. Casson fluid has been studied a lot since it has specific usefulness. Many businesses, including as food processing, polymer technology, medicines, and material manufacturing, need to know how this fluid moves heat and mass. To get accurate results, modeling and testing must be done correctly. The main purpose of this study is to look at how heat and mass transfer work in a magnetohydrodynamic (MHD) Casson fluid flow model, where the fluid moves down an infinitely long vertical surface that is affected by an external magnetic field and chemical reactions. This research is predicated on various prior investigations that have motivated the present inquiry. Nazeer et al. in 2009 conducted a theoretical examination of the impacts of the electrical double layer in multiphase flows, concentrating on Jeffrey fluids, a kind of Non-Newtonian fluid, traversing lubricated diverging channels. Omar et al. in 2022 investigated the Hall and Soret effects in unsteady magnetohydrodynamic fluid flow via rotating porous media, taking into account heat radiation and chemical processes in a second-grade nanofluid demonstrating shear-thickening and thinning characteristics. This study elucidated the influence of Soret effects, chemical processes, and heat radiation on fluid dynamics. Mustafa et al. in 2011 examined the boundary layers of Casson fluid in impulsive motion over a flat sheet, which subsequently prompted further research on MHD Casson fluid flow influenced by thermal radiation effects by Bhattacharyya in 2013. Vijaya and Reddy investigated the magnetohydrodynamic flow of Casson fluid over vertical porous plates, taking into account factors such as chemical reactions, Soret effects, and heat radiation. Other important studies have looked at heat and mass transfer in non-Newtonian nanofluids over extending sheets with different heat sources and viscosities by Santhoshi et al. in 2018, unsteady MHD flow in permeable channels by Kallepalli et al., and numerical analyses of viscoelastic fluid flow over porous plates by Sivaiah et al., in 2019. Subsequent investigations have concentrated on the synergistic effects of Soret and Dufour phenomena in micropolar fluids traversing stretching sheets within porous media, alongside the influences of chemical processes and heat radiation on nonlinear MHD nanofluids over intricate geometries by Sujatha et al., Ibrahim et al. Research has been undertaken on mixed convection flows affected by magnetic fields and heat radiation by Kumar et al.Furthermore, recent research conducted by Padmavathi et al. (2022) on mass transfer in mucus fluids subjected to pulsatile flow and electromagnetic fields has catalyzed investigations in biomedical fluid dynamics. Research conducted by Abbas Yusuf Balarabe et al. and Farhan Ali et al. (2023) has examined heat and mass transfer in unsteady magnetohydrodynamic (MHD) flows of second-grade and Casson fluids, respectively. These studies incorporated parameters such as thermal

Received: July 14, 2025

International Journal of Applied Mathematics

Volume 38 No. 1s, 2025

ISSN: 1311-1728 (printed version); ISSN: 1314-8060 (on-line version)

radiation, heat sources, Prandtl and Schmidt numbers, with the initial flow induced by external magnetic fields.

This study enhances prior models by incorporating chemical reaction effects and the Dufour effect—where concentration gradients affect temperature fields—into the governing equations, reflecting the growing significance of the Dufour effect. A comprehensive analysis of fluid flow over an exponentially infinite vertical surface subjected to an applied magnetic field is conducted. By using the right non-dimensional variables, the governing equations and boundary conditions can be changed into non-dimensional forms. Laplace transformations provide us analytical solutions for the momentum, energy, and concentration fields of the Casson fluid. MATLAB is used to show the results in graphs, and there are thorough talks of skin friction, Sherwood number, and Nusselt number, with graphs to back it up.

MATHEMATICAL FORMULATION:

Let us investigate the MHD Casson fluid with existence of the influence of dufour, thermal radiation, heat source and the chemically reactive fluid flow through a vertical surface. Initially when the demonstration takes place, the velocity profile is taken under consideration. Additionally, the magnetic strength of the field is considered in the opposite *x*-axis. Further, when t = 0, the velocity is U = e^{at} for all the above stated conditions, the initial governing equations are derived from the Boussinesq's approximation. Where u denotes velocity constituent in x-axis and v denotes velocity constituent in y-axis. The flow is in accordance with the kinematic viscosity is denoted as v, T is the Temperature of fluid and T_∞ is the ambient temperature and the concentration field is C and C_∞ is the ambient concentration. ρ denotes the fluid density, t denotes time, the magnetic field is denoted as B_0 and electrical conductivity of the fluid is given as σ.

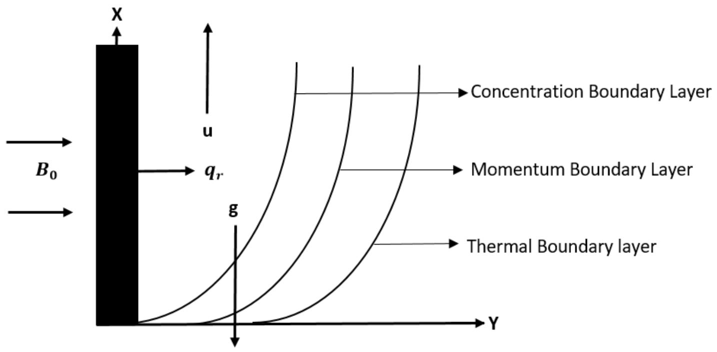

Figure : 1

Therefore the respective governing equations are as follows

Momentum equation:

$$\frac{\partial u}{\partial t'} = g\beta'(T - T_\infty) + g\beta^*(C - C_\infty) + v\left(1 + \frac{1}{\beta}\right)\frac{\partial^2 u}{\partial y^2} - \frac{\sigma B_0^2}{\rho}u \quad (1)$$

Received: July 14, 2025

International Journal of Applied Mathematics

Volume 38 No. 1s, 2025

ISSN: 1311-1728 (printed version); ISSN: 1314-8060 (on-line version)

Energy equation:

$$\rho C_p \frac{\partial T}{\partial t'} = k\frac{\partial^2 T}{\partial y^2} - Q_0(T - T_\infty) - \frac{\partial q_r}{\partial y} + \frac{D_T K_T}{C_S}\frac{\partial^2 C}{\partial y^2} \tag{2}$$

Concentration equation:

$$\frac{\partial C}{\partial t'} = D\frac{\partial^2 C}{\partial y^2} - Kr\,(C - C_\infty) \tag{3}$$

The boundary conditions are

$$\left.\begin{array}{llll} u = 0, & T = T_\infty, & C = C_\infty & \text{for all } y \text{ and } t' \geq 0 \\ u = u_0, & T = T_W, & C = C_W & \text{at } y = 0 \\ u = 0, & T = T_W, & C = C_W & \text{at } y \to 0 \end{array}\right\} \tag{4}$$

Local gradient:

$$\frac{\partial q_r}{\partial y} = -4b^*\sigma\,(T_\infty^4 - T^4) \tag{5}$$

By implying Taylor's theorem and eliminating higher order terms, we get

$$T^4 \cong 4T_\infty^3\,T - 3T_\infty^4 \tag{6}$$

By using the equation (5) and (6) in equation (2), it becomes

$$\rho C_p\frac{\partial T}{\partial t'} = K\frac{\partial^2 T}{\partial y^2} - Q_0(T - T_\infty) - 16b^*\sigma T_\infty^3(T - T_\infty) \tag{7}$$

Non-Dimensional variables are as follows:

$$U = \frac{u}{u_0}; \quad t = \frac{t' u_0^2}{v}; \quad Y = \frac{y u_0}{v}; \quad S_c = \frac{v}{D};$$

$$\theta = \frac{T - T_\infty}{T_W - T_\infty}; \quad \varphi = \frac{C - C_\infty}{C_W - C_\infty}; \quad Gr = \frac{gv\beta'(T_W - T_\infty)}{u_0^3}; \quad Gc = \frac{gv\beta^*(C_W - C_\infty)}{u_0^3};$$

$$Kr = \frac{Ku_0^2}{v}; \quad Rd = \frac{16\sigma b^* v^2 T_\infty^3}{ku_0^2}; \quad Pr = \frac{\rho v C_p}{k}; \quad Du = \frac{D_T K_T}{C_S\,\rho C_p}\frac{C_W - C_\infty}{T_W - T_\infty}$$

Implementing the Non-Dimensional quantities in equations (1), (3) and (7)

$$\frac{\partial U}{\partial t} = \left(1 + \frac{1}{\beta}\right)\frac{\partial^2 U}{\partial Y^2} + Gr\theta + Gc\varphi - MU \tag{8}$$

$$\frac{\partial \theta}{\partial t} = \frac{1}{P_r}\frac{\partial^2 \theta}{\partial Y^2} - Q\theta - Rd\theta + Du\frac{\partial^2 \varphi}{\partial Y^2} \tag{9}$$

$$\frac{\partial \varphi}{\partial t} = \frac{1}{S_c}\frac{\partial^2 \varphi}{\partial Y^2} - K\varphi \tag{10}$$

Received: July 14, 2025

Volume 38 No. 1s, 2025

ISSN: 1311-1728 (printed version); ISSN: 1314-8060 (on-line version)

The boundary conditions:

$U = 0; \quad \theta = 0; \quad \varphi = 0; \quad for\ all\ Y\ and\ t \leq 0$

$U = e^{at}; \quad \theta = 1; \quad \varphi = 1; \quad at\ Y = 0$

$U \to 0; \quad \theta \to 0; \quad \varphi \to 0; \quad at\ Y \to \infty$

We can now acquire the solution for the flow model by incorporating the technique of Laplace Transformation with respect to time in the equations (8), (9) and (10). Hence the resultant Laplace equations are as follows:

$$\begin{aligned}
\mathrm{L(U)} = \; & \frac{e^{-y\sqrt{\frac{s+M}{\beta_0}}}}{s} - \mathrm{Gc}\frac{R_1}{R_2}\left[\frac{e^{-y\sqrt{\mathrm{Sc}\,(s+K)}}}{s}\right] + \mathrm{Gc}\frac{R_1}{R_2}\left[\frac{e^{-y\sqrt{\mathrm{Sc}\,(s+K)}}}{s+R_2}\right] - \mathrm{Gr}\frac{R_3}{R_4}\left[\frac{e^{-y\sqrt{\mathrm{Pr}\,(s+\alpha)}}}{s}\right] \\
& + \mathrm{Gr}\frac{R_3}{R_4}\left[\frac{e^{-y\sqrt{\mathrm{Pr}\,(s+\alpha)}}}{s+R_4}\right] - \mathrm{Gr}\frac{R_1}{R_2}(\mathrm{Sc.K} + \mathrm{Sc.s})\left[\frac{e^{-y\sqrt{\mathrm{Sc}\,(s+K)}}}{s}\right] \\
& + \mathrm{Gr}\frac{R_1}{R_2}(\mathrm{Sc.K} + \mathrm{Sc.s})\left[\frac{e^{-y\sqrt{\mathrm{Sc}\,(s+K)}}}{s+R_2}\right] - \mathrm{Gr.Du}\frac{R_3}{R_4}(\mathrm{Pr.s} + \mathrm{Pr.\alpha})\left[\frac{e^{-y\sqrt{\mathrm{Pr}\,(s+\alpha)}}}{s}\right] \\
& + \mathrm{Gr.Du}\frac{R_3}{R_4}(\mathrm{Pr.s} + \mathrm{Pr.\alpha})\left[\frac{e^{-y\sqrt{\mathrm{Pr}\,(s+\alpha)}}}{s+R_4}\right] \qquad (11)
\end{aligned}$$

$$\begin{aligned}
\mathrm{L(\theta)} = \; & \left[\frac{e^{-y\sqrt{\mathrm{Pr}\,(s+\alpha)}}}{s}\right] + \mathrm{Du}\frac{q_1}{q_2}\left[\frac{e^{-y\sqrt{\mathrm{Sc}\,(s+K)}}}{s}\right] - \mathrm{Du}\frac{q_1}{q_2}\left[\frac{e^{-y\sqrt{\mathrm{Sc}\,(s+K)}}}{s+q_2}\right] \\
& + \mathrm{Du}\frac{q_3}{q_4}\left[\frac{e^{-y\sqrt{\mathrm{Sc}\,(s+K)}}}{s}\right] - \mathrm{Du}\frac{q_3}{q_4}\left[\frac{e^{-y\sqrt{\mathrm{Sc}\,(s+K)}}}{s+q_4}\right] \qquad (12)
\end{aligned}$$

$$\mathrm{L(\varphi)} = \left[\frac{e^{-y\sqrt{\mathrm{Sc}\,(s+K)}}}{s}\right] \qquad (13)$$

Following these Laplace equations, the final solutions of the equations (11), (12) and (13) are attained by incorporating the Inverse Laplace transforms. The resulting solutions are as follows:

$$\varphi = \frac{e^{kt}}{2}\left[e^{-y\sqrt{Sc.k}}\, erfc\left(\eta\sqrt{Sc} - \sqrt{kt}\right) + e^{y\sqrt{Sc.k}}\, erfc\left(\eta\sqrt{Sc} + \sqrt{kt}\right)\right] \qquad (14)$$

Received: July 14, 2025

International Journal of Applied Mathematics

Volume 38 No. 1s, 2025

ISSN: 1311-1728 (printed version); ISSN: 1314-8060 (on-line version)

$$\theta = \frac{e^{\alpha t}}{2}\left[e^{-y\sqrt{Pr.\alpha}}\, erfc\left(\eta\sqrt{Pr} - \sqrt{\alpha t}\right) + e^{y\sqrt{Pr.\alpha}}\, erfc\left(\eta\sqrt{Pr} + \sqrt{\alpha t}\right)\right]$$
$$+ Du\,\frac{q_1}{q_2}\,\frac{e^{kt}}{2}\left[e^{-y\sqrt{Sc.k}}\, erfc\left(\eta\sqrt{Sc} - \sqrt{kt}\right) + e^{y\sqrt{Sc.k}}\, erfc\left(\eta\sqrt{Sc} + \sqrt{kt}\right)\right]$$
$$- Du\,\frac{q_1}{q_2}\,\frac{e^{(k-q_2)t}}{2}\left[e^{-y\sqrt{Sc(k-q_2)}}\, erfc\left(\eta\sqrt{Sc} - \sqrt{(k-q_2)t}\right)\right.$$
$$\left. + e^{y\sqrt{Sc(k-q_2)}}\, erfc\left(\eta\sqrt{Sc} + \sqrt{(k-q_2)t}\right)\right]$$
$$- Du\frac{q_3}{q_4}\frac{e^{\alpha t}}{2}\left[e^{-y\sqrt{Pr.\alpha}}\, erfc\left(\eta\sqrt{Pr} - \sqrt{\alpha t}\right) + e^{y\sqrt{Pr.\alpha}}\, erfc\left(\eta\sqrt{Pr} + \sqrt{\alpha t}\right)\right]$$
$$+ Du\frac{q_3}{q_4}\frac{e^{(\alpha-q_4)t}}{2}\left[e^{-y\sqrt{\mathrm{Pr}(\alpha-q_4)}}\, erfc\left(\eta\sqrt{Pr} - \sqrt{(\alpha-q_4)t}\right)\right.$$
$$+ e^{y\sqrt{\mathrm{Pr}(\alpha-q_4)}}\, erfc\left(\eta\sqrt{Pr}\right.$$
$$\left.\left. + \sqrt{(\alpha-q_4)t}\right)\right] \qquad (15)$$

Received: July 14, 2025

International Journal of Applied Mathematics

Volume 38 No. 1s, 2025

ISSN: 1311-1728 (printed version); ISSN: 1314-8060 (on-line version)

$$U = \frac{e^{Mt}}{2}\left[e^{-y\sqrt{\frac{M}{\beta_0}}} erfc\left(\frac{\eta}{\sqrt{\beta_0}} - \sqrt{Mt}\right) + e^{y\sqrt{\frac{M}{\beta_0}}} erfc\left(\frac{\eta}{\sqrt{\beta_0}} + \sqrt{Mt}\right)\right]$$
$$- \mathrm{Gc}\frac{\mathrm{R}_1}{\mathrm{R}_2}\frac{e^{kt}}{2}\left[e^{-y\sqrt{Sc.k}} erfc\left(\eta\sqrt{Sc} - \sqrt{kt}\right) + e^{y\sqrt{Sc.k}} erfc\left(\eta\sqrt{Sc} + \sqrt{kt}\right)\right]$$
$$+ \mathrm{Gc}\frac{\mathrm{R}_1}{\mathrm{R}_2}\frac{e^{(k-\mathrm{R}_2)t}}{2}\left[e^{-y\sqrt{Sc(k-\mathrm{R}_2)}} erfc\left(\eta\sqrt{Sc} - \sqrt{(k-R_2)t}\right)\right.$$
$$\left. + e^{y\sqrt{Sc(k-\mathrm{R}_2)}} erfc\left(\eta\sqrt{Sc} + \sqrt{(k-\mathrm{R}_2)t}\right)\right]$$
$$- \mathrm{Gr}\frac{\mathrm{R}_3}{\mathrm{R}_4}\frac{e^{\alpha t}}{2}\left[e^{-y\sqrt{Pr.\alpha}} erfc\left(\eta\sqrt{Pr} - \sqrt{\alpha t}\right) + e^{y\sqrt{Pr.\alpha}} erfc\left(\eta\sqrt{Pr} + \sqrt{\alpha t}\right)\right]$$
$$+ \mathrm{Gr}\frac{\mathrm{R}_3}{\mathrm{R}_4}\frac{e^{(\alpha-\mathrm{R}_4)t}}{2}\left[e^{-y\sqrt{\mathrm{Pr}(\alpha-\mathrm{R}_4)}} erfc\left(\eta\sqrt{Pr} - \sqrt{(\alpha-\mathrm{R}_4)t}\right)\right.$$
$$\left. + e^{y\sqrt{\mathrm{Pr}(\alpha-\mathrm{R}_4)}} erfc\left(\eta\sqrt{Pr} + \sqrt{(\alpha-\mathrm{R}_4)t}\right)\right]$$
$$- \mathrm{Gr}\frac{\mathrm{R}_1}{\mathrm{R}_2}(Sc.k + Sc.s)\frac{e^{kt}}{2}\left[e^{-y\sqrt{Sc.k}} erfc\left(\eta\sqrt{Sc} - \sqrt{kt}\right)\right.$$
$$\left. + e^{y\sqrt{Sc.k}} erfc\left(\eta\sqrt{Sc} + \sqrt{kt}\right)\right]$$
$$+ \mathrm{Gr}\frac{\mathrm{R}_1}{\mathrm{R}_2}(Sc.k + Sc.s)\frac{e^{(k+R_2)t}}{2}\left[e^{-y\sqrt{Sc(k+R_2)}} erfc\left(\eta\sqrt{Sc} - \sqrt{(k+R_2)t}\right)\right.$$
$$\left. + e^{y\sqrt{Sc(k+R_2)}} erfc\left(\eta\sqrt{Sc} + \sqrt{(k+R_2)t}\right)\right]$$
$$- Gr.Du\frac{\mathrm{R}_3}{\mathrm{R}_4}(Pr.s + Pr.\alpha)\frac{e^{\alpha t}}{2}\left[e^{-y\sqrt{Pr.\alpha}} erfc\left(\eta\sqrt{Pr} - \sqrt{\alpha t}\right)\right.$$
$$\left. + e^{y\sqrt{Pr.\alpha}} erfc\left(\eta\sqrt{Pr} + \sqrt{\alpha t}\right)\right]$$
$$+ Gr.Du\frac{\mathrm{R}_3}{\mathrm{R}_4}(Pr.s + Pr.\alpha)\frac{e^{(\alpha-\mathrm{R}_4)t}}{2}\left[e^{-y\sqrt{\mathrm{Pr}(\alpha-\mathrm{R}_4)}} erfc\left(\eta\sqrt{Pr} - \sqrt{(\alpha-\mathrm{R}_4)t}\right)\right.$$
$$\left. + e^{y\sqrt{\mathrm{Pr}(\alpha-\mathrm{R}_4)}} erfc\left(\eta\sqrt{Pr} + \sqrt{(\alpha-\mathrm{R}_4)t}\right)\right] \quad (16)$$

RESULT AND DISCUSSIONS:

The method of Laplace transformation has been implied to solve the described flow model and the solution is obtained. The solutions are analysed using MATLAB software and the consequences of all the parameters in three fields has been analysed.

Received: July 14, 2025

International Journal of Applied Mathematics

Volume 38 No. 1s, 2025

ISSN: 1311-1728 (printed version); ISSN: 1314-8060 (on-line version)

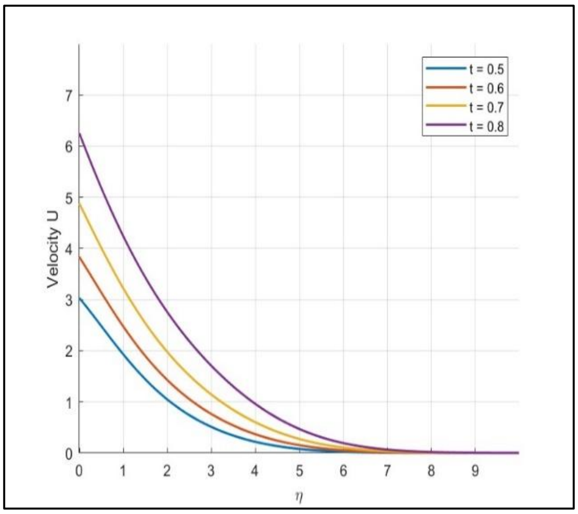

Fig:2

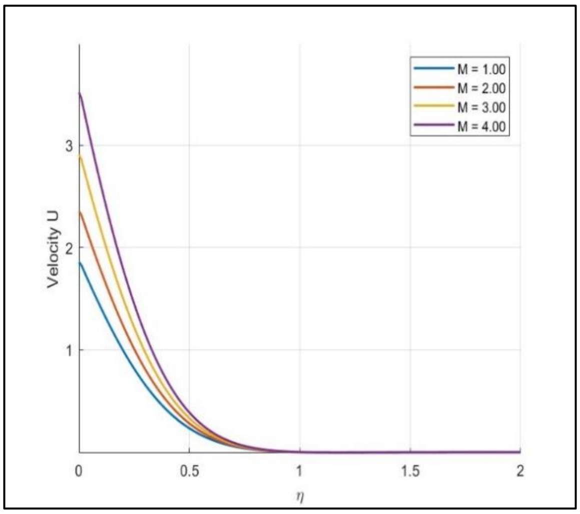

Fig:3

Addition to this, Governing parameters including Skin friction, Nusselt number and Sherwood number have been solved and the resulting solution has been graphically analysed. Graphical investigation is executed to visualize how various parameters influenced the fluid flow.Figure:2 Represents the time fluctuation over the fluid velocity and Figure:3 shows the consequence of Magnetic strength parameter on the velocity field. It is visible that when the time enlarges, the momentum boundary layer also increases. Similarly the Momentum boundary layer increments along with the Magnetic field of the fluid flow. Physically, when the Magnetic field is induced into a fluid flow with ability of conduction it results in inducing a Magnetic Lorentz force. As a consequence the fluid velocity increases.

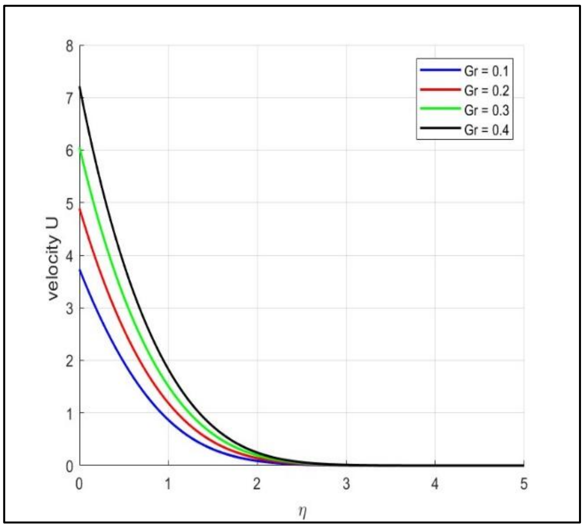

Fig:4

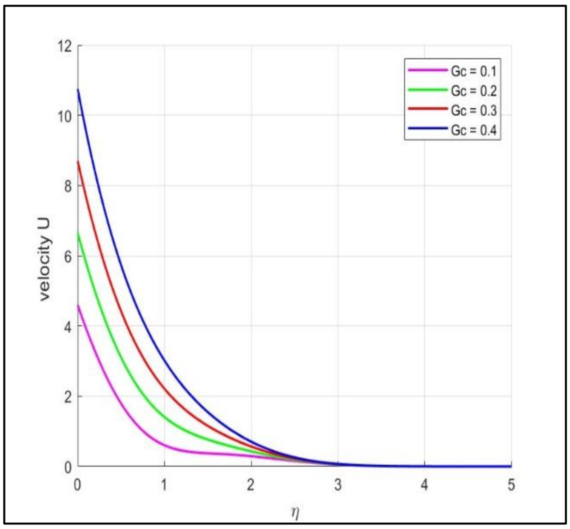

Fig:5

Figure:4 and 5 represents the consequence of Gr and Gc in the velocity field. Both the Thermal and mass grashof number elevates the fluid velocity with the increase in Gr and Gc values. The shows the clear evidence of buoyancy forces becoming more significantly prompting an elevation in fluid velocity.

Received: July 14, 2025

International Journal of Applied Mathematics

Volume 38 No. 1s, 2025

ISSN: 1311-1728 (printed version); ISSN: 1314-8060 (on-line version)

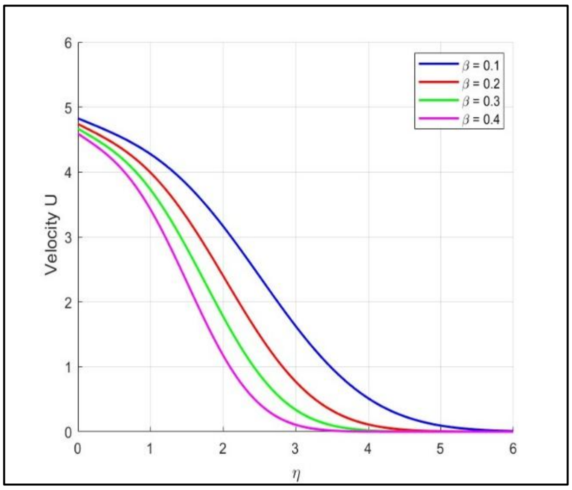

Fig:6

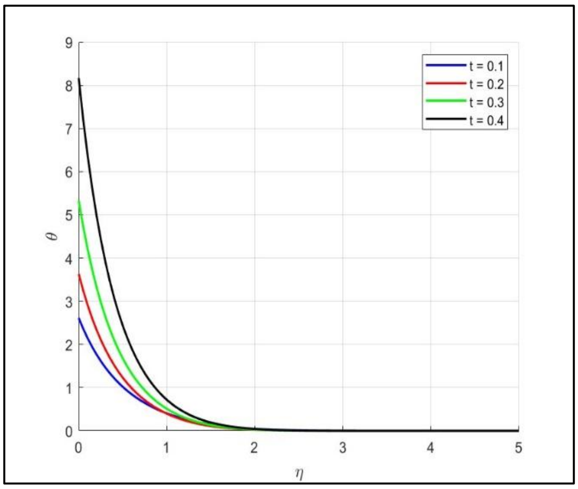

Fig: 7

Figure: 6 elucidates the impact of casson fluid parameter (β). The graph visualizes that as the casson parameter is inclined, the fluid velocity declines rapidly. Since the casson parameter is inversely related to the yield stress, the velocity field declines because there is a reduction in fluid's resistivity to flow thus supressing the velocity of the fluid. Figure:7-11 brings out the repercussion of various parameters in the temperature fields. Parameters like Prandtl number, Thermal radiation, Heat source and Dufour effect has significant impact in the temperature field. From figure:7 it is visible that as the t value uplifts the temperature of the fluid increases rapidly.

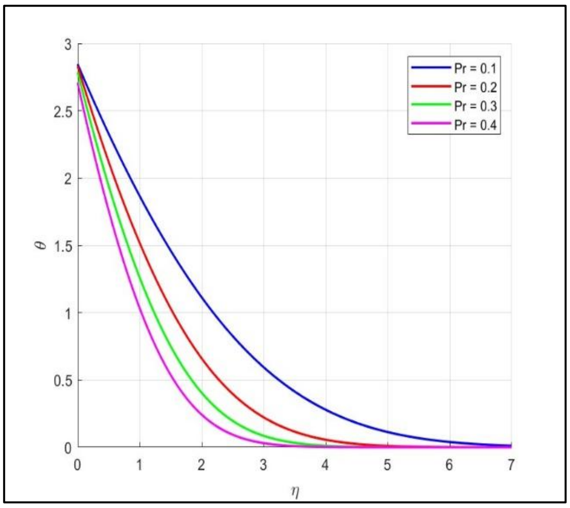

Fig:8

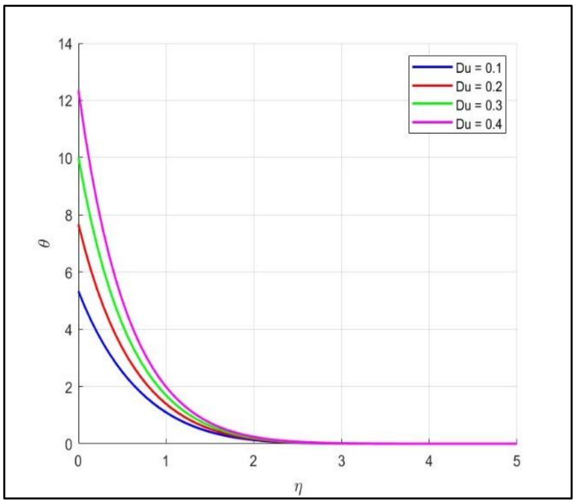

Fig:9

Figure: 8 exhibits the declination of temperature when there is an increament in the prandtl number. As the prandtl number increments, Thermal diffusivity declines which in turn reduces the heat transfer relative to the momentum. Fig: 8 examines the effect of dufour in the temperature profile. Dufour effect is the heat flow caused by the Concentration profile in the MHD casson fluid flow. The dufour effect increases a heat flux in the flow system due to concentration field which leads to effective addition of enrgy into the system. Therfore the Teemperature increases with the increase in dufour effect.

Received: July 14, 2025

International Journal of Applied Mathematics

Volume 38 No. 1s, 2025

ISSN: 1311-1728 (printed version); ISSN: 1314-8060 (on-line version)

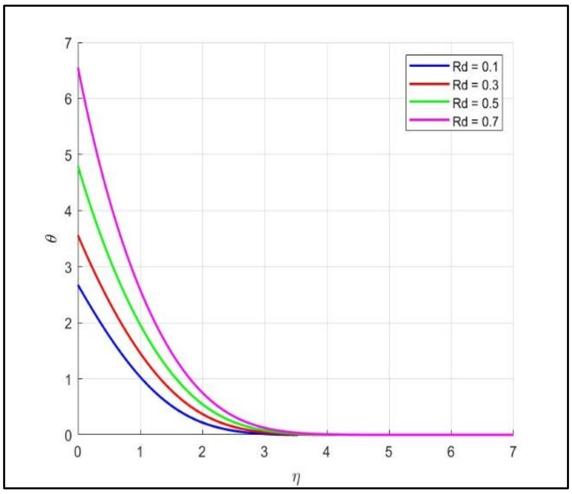

Fig:10

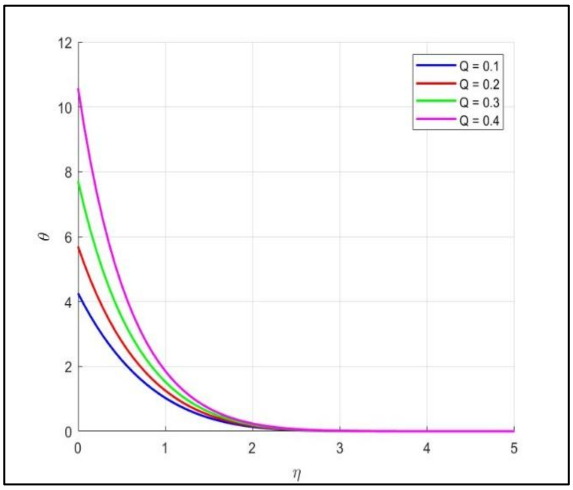

Fig:11

Figure:10 brings out the effect of Thermal radiation caused in the Temperature profile. And Figure: 11 shows the impact of Heat sources in the temperature field. It is apparent that the Temperature upsurges rapidly with an delibrant raise in thermal radiation and as well as the Heat sources. Owing to the thermal absorption capacity of the MHD Casson fluid, the temperature inclines with the increment of Thermal radiation. Similarly, when an external heat source is being introduced in the fluid flow system the fluid particles are transferred rapidly and the energy level increases which results in the increase of the temperature. Figure:12-14 visualizes the implementation of various parameters such as Schmidt number and chemical reaction in the Concentration fields.

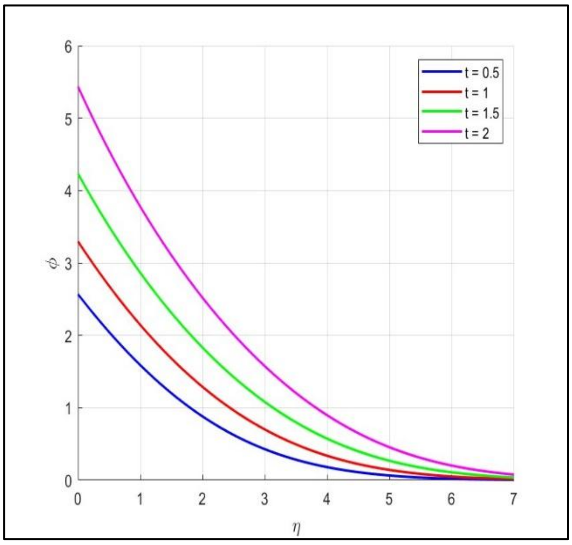

Fig: 12

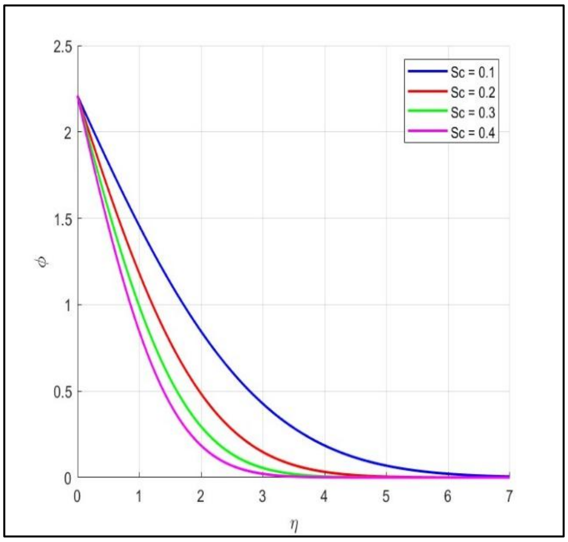

Fig:13

Analysing the graphicall representations of the concentration fields, we have arrived at the result such that the Concentration profile devolops significantly with the increase of ‘t’. From figure: 13, it is evident that there is a deterioriation in concentration level when there is increase in Schmidt number. When the schmidt number increases, it leads to an effective momentum diffusion. As a result the concentration boundary layer becomes more slender. Figure: 14 brings

Received: July 14, 2025

International Journal of Applied Mathematics

Volume 38 No. 1s, 2025

ISSN: 1311-1728 (printed version); ISSN: 1314-8060 (on-line version)

out the impact of chemical reaction in the concentration profile. As the chemical reaction rate increases, more number of particle involves in chemical reaction which means the diffusion rate increases rapidly resulting in the upsurge of concentration profile.

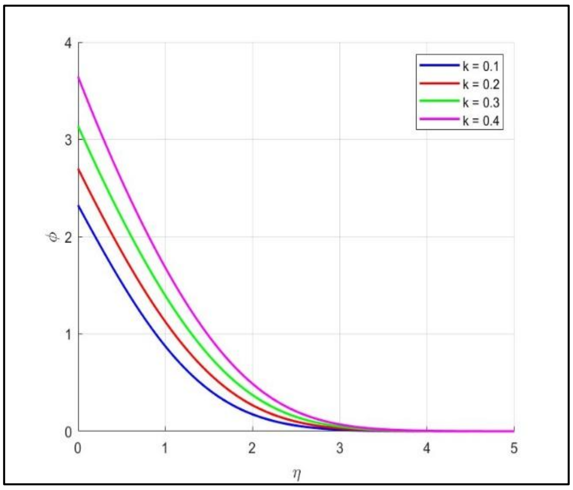

Fig:14

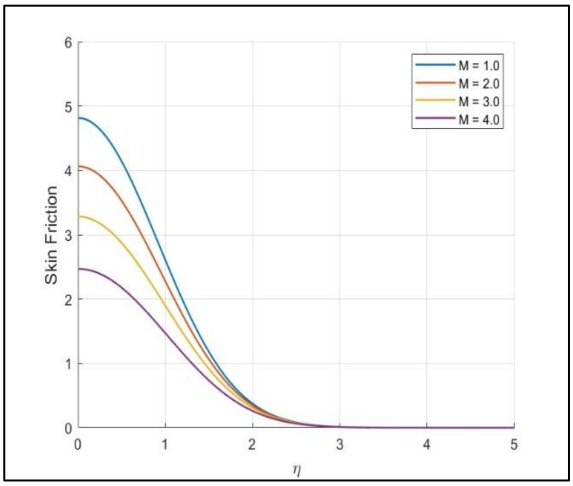

Fig:15

From figure: 14 it is clear that the chemical reaction induces the Concentration profile considerably. From Fig:15-17, the impact of Skin friction caused by various parameters like Magnetic field parameter (M), Grashof number (Gr and Gc) have been analysed. Fig: 15 shows that there is a decrease in the Skin friction level when there is a increases in the externaly applied Magnetic field. Figure:16 shows the enhancement of Skin friction in the fluid flow system when there is an increase in thermal grashof number (Gr) as well as the mass grashof number (Gc). It is evident that as the grashof numbers increse, a stronger buoyancy force intensifies the flow and increases the shear stress at the surface which leads to the increase of Skin friction. Following figure: 18,19 elucidates the aftermath of Nusselt number and Sherwood number.

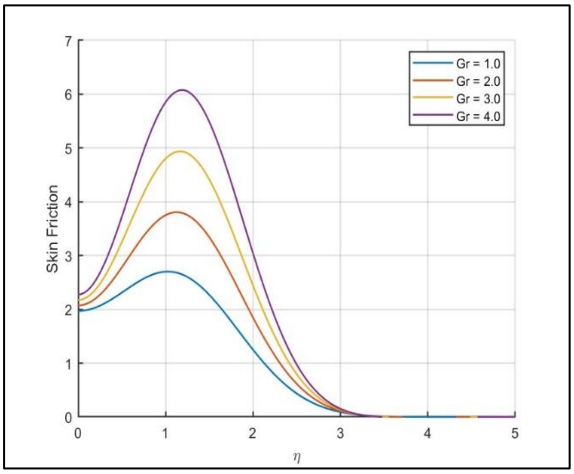

Fig: 16

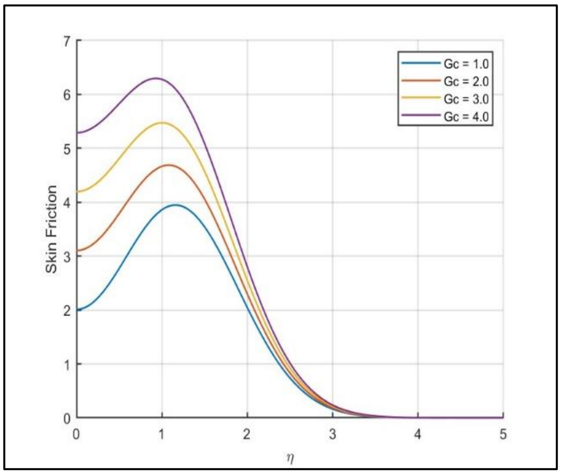

Fig:17

Figure: 18 shows the Changes undergone by the Nusselt number due to tha effect of Prandtl number. It is visible that the Nusselt number levels up with respect to Prandtl number. Evidentically the higher Pr inducates a thinner boundary layer which enhances the heat transfer

Received: July 14, 2025

International Journal of Applied Mathematics

Volume 38 No. 1s, 2025

ISSN: 1311-1728 (printed version); ISSN: 1314-8060 (on-line version)

of the fluid in the system. As a resulting effect of enhanced heat transfer, the nusselt number also increases. Figure:19 exhibits the impact of chemical reaction in sherwood number. It is visibile that chemical reaction parameter (k) highly enhances the Sherwood number.

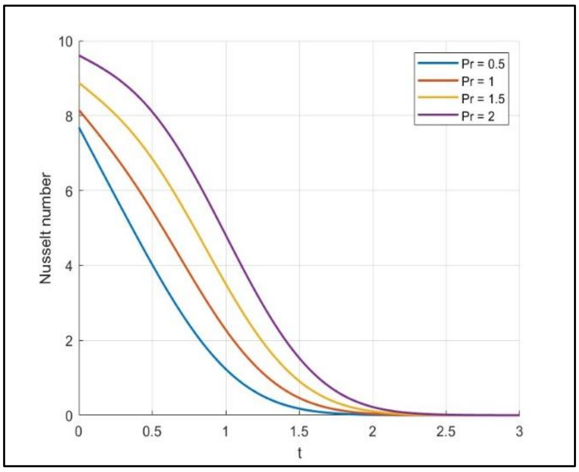

Fig: 18

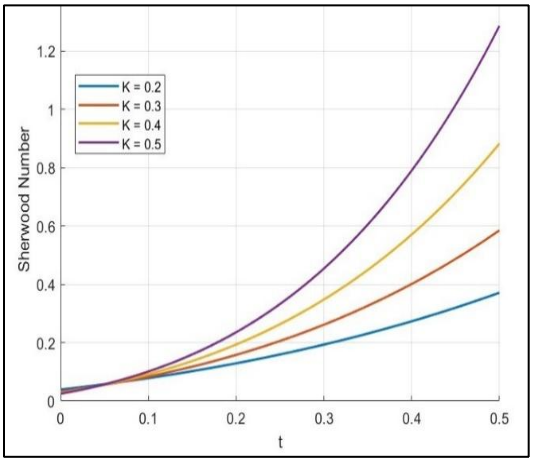

Fig: 19

CONCLUSION:

This study furnishes approximate analytical solutions for a MHD casson fluid through an upright surface with occurrence of Thermal radiation, Chemical reaction and Dufour effect. We have arrived at the solutions for dimensionless velocity, temperature and concentration by deploying the method of Laplace transforms. The parameters of all the fields including Skin friction, Nusselt number and Sherwood number are portrayed through graphs.

- Magnetic field upsurges the velocity field.
- Velocity drops with increment of casson parameter.
- (Gr)Thermal grashof number uplifts the fluid velocity.
- (Gc)Mass grashof number also claims to raise the velocity of the fluid.
- Temperature enhances with the rise of thermal radiation.
- Increment in Heat source results in rapid uplifting of Temperature field.
- When there is an increase in Prandtl number temperature profile declines rapidly.
- Temperature profile falls with an rise in Prandlt number.
- Dufour effect (Du) induces the Temperature profile considerably.
- Concentration profile falls with the impact of Schmidt number.
- Enlargement in Chemical reaction leads to the decline of concentration profile.
- Graphical study justifies the study of all fields of the casson fluid.

Received: July 14, 2025

International Journal of Applied Mathematics

Volume 38 No. 1s, 2025

ISSN: 1311-1728 (printed version); ISSN: 1314-8060 (on-line version)

APPENDIX:

$\alpha \quad = Rd + Q$

$\beta_0 \; = \left(1 + \frac{1}{\beta}\right)$

$\eta \; = \; \frac{Y}{2\sqrt{t}}$

$$q_1 = \frac{\Pr\,(Sc.k + Sc.s)}{(Sc - Pr)}$$

$$q_2 = \frac{Sc.k - Pr.\alpha}{Sc - Pr}$$

$$q_3 = \frac{\Pr\,(Pr.s + Pr.\alpha)}{\Pr - Sc}$$

$$q_4 = \frac{Pr.\alpha - Sc.k}{\Pr - Sc}$$

$$R_1 = \frac{1}{Sc.\beta_0 - 1}$$

$$R_2 = \frac{Sc.k.\beta_0 - M}{Sc.\beta_0 - 1}$$

$$R_3 = \frac{1}{Pr.\beta_0 - 1}$$

$$R_4 = \frac{Pr.\alpha.\beta_0 - M}{Pr.\beta_0 - 1}$$

Sherwood Number $= \left[\frac{\partial\varphi}{\partial Y}\right]_{Y=0}$

$$= -\frac{Sc\sqrt{k}}{\sqrt{\pi t}} e^{kt/2}(e^{-kt} + 1)$$

Nusselt Number $= \left[\frac{\partial\theta}{\partial Y}\right]_{Y=0}$

$$-\frac{1}{\sqrt{\pi t}}[e^{\frac{\alpha t}{2}}\left(\Pr\sqrt{\alpha}e^{-\alpha t} + \Pr\sqrt{\alpha}\right) + Du\frac{q_1}{q_2}e^{\frac{kt}{2}}(Sc\sqrt{k}e^{-kt} + Sc\sqrt{k})$$
$$-Du\frac{q_1}{q_2}e^{\frac{(k-q_2)t}{2}}(Sc\sqrt{k-q_2}e^{-(k-q_2)t} + Sc\sqrt{k-q_2})$$
$$-Du\frac{q_3}{q_4}e^{\frac{\alpha t}{2}}(\Pr\sqrt{\alpha}e^{-\alpha t} + \Pr\sqrt{\alpha})$$
$$+Du\frac{q_3}{q_4}e^{\frac{(\alpha-q_4)t}{2}}(\Pr\sqrt{\alpha-q_4}e^{-(\alpha-q_4)t} + \Pr\sqrt{\alpha-q_4})]$$

Skin Friction $= \left[\frac{\partial U}{\partial Y}\right]_{Y=0}$

Received: July 14, 2025

International Journal of Applied Mathematics

Volume 38 No. 1s, 2025

ISSN: 1311-1728 (printed version); ISSN: 1314-8060 (on-line version)

$$\frac{e^{Mt}}{2}\sqrt{\frac{M}{\beta_0}}\left[\,erfc\left(\frac{\eta}{\sqrt{\beta_0}}+\sqrt{Mt}\right)-\ erfc\left(\frac{\eta}{\sqrt{\beta_0}}-\sqrt{Mt}\right)\right]$$

$$-\mathrm{Gc}\frac{\mathrm{R}_1}{\mathrm{R}_2}\frac{e^{kt}}{2}\sqrt{Sck}\left[\,erfc\left(\eta\sqrt{Sc}+\ \sqrt{kt}\right)-\ \ erfc\left(\eta\sqrt{Sc}-\ \sqrt{kt}\right)\right]$$

$$+\ \mathrm{Gc}\frac{\mathrm{R}_1}{\mathrm{R}_2}\frac{e^{(k-\mathrm{R}_2)t}}{2}\sqrt{Sc(k-\mathrm{R}_2)}\left[erfc\left(\eta\sqrt{Sc}+\sqrt{(k-R_2)t}\right)\right.$$

$$\left.-\ erfc\left(\eta\sqrt{Sc}-\ \sqrt{(k-\mathrm{R}_2)t}\right)\right]$$

$$+\mathrm{Gr}\frac{\mathrm{R}_3}{\mathrm{R}_4}\frac{e^{(\alpha-\mathrm{R}_4)t}}{2}\sqrt{\mathrm{Pr}(\alpha-\mathrm{R}_4)}\ \left[erfc\left(\eta\sqrt{Pr}+\sqrt{(\alpha-\mathrm{R}_4)t}\right)\right.$$

$$\left.-\ erfc\left(\eta\sqrt{Pr}+\ \sqrt{(\alpha-\mathrm{R}_4)t}\right)\right]$$

$$-\ \mathrm{Gr}\frac{\mathrm{R}_1}{\mathrm{R}_2}(Sck+Sc\ s)\frac{e^{kt}}{2}\sqrt{Sc\ k}\left[\,erfc\left(\eta\sqrt{Sc}+\sqrt{kt}\right)-\ erfc\left(\eta\sqrt{Sc}-\sqrt{kt}\right)\right]$$

$$+\ \mathrm{Gr}\frac{\mathrm{R}_1}{\mathrm{R}_2}(Sck+Sc\ s)\frac{e^{(k+R_2)t}}{2}\sqrt{Sc(k+R_{2)}}\left[erfc-erfc\left(\eta\sqrt{Sc}-\ \sqrt{(k+R_{2)}t)}\right)\right]$$

$$-\ Gr\ Du\frac{\mathrm{R}_3}{\mathrm{R}_4}(Prs+Pr\alpha)\frac{e^{\alpha t}}{2}\sqrt{Pr\ \alpha}\ \left[erfc\left(\eta\sqrt{Pr}+\ \sqrt{\alpha t}\right)-\ erfc\left(\eta\sqrt{Pr}-\ \sqrt{\alpha t}\right)\right]$$

$$+Gr\ Du\frac{\mathrm{R}_3}{\mathrm{R}_4}(Prs+Pr\alpha)\frac{e^{(\alpha-\mathrm{R}_4)t}}{2}\sqrt{\mathrm{Pr}(\alpha-\mathrm{R}_4)}\left[erfc\left(\eta\sqrt{Pr}+\ \sqrt{(\alpha-\mathrm{R}_4)t}\right)-\right.$$

$$\left.\left(\eta\sqrt{Pr}+\ \sqrt{(\alpha-\mathrm{R}_4)t}\right)\right]$$

REFFERENCES:

[1] Nazeer, M.; Hussain, F.; Khan, M. I.; Khalid, K. Theoretical Analysis of Electrical Double Layer Effects on the Multiphase Flow of Jeffrey Fluid Through a Divergent Channel with Lubricated Walls. Waves Random Motion Complex Media 2022, 39.

[2] Omar, B. T.; Raghunath, K.; Ali, F.; Khalid, M.; Tag ElDin, M.; Oreijah, M.; Guedri, K.; Khedher, N. B.; Khan, M. I. Hall Current and Soret Effects on Unsteady MHD Rotating Flow of Second-Grade Fluid Through Porous Media Under the Influences of Thermal Radiation and Chemical Reactions. Catalysts 2022, 12.

[3] Mustafa, M.; Hayat, T.; Pop, I.; Aziz, A. Unsteady Boundary Layer Flow of a Casson Fluid Due to an Impulsively Started Moving Flat Plate. Heat Transf. Asian Res. 2011, 40, 563–576.

[4] Bhattacharyya, K. MHD Stagnation-Point Flow of Casson Fluid and Heat Transfer Over a Stretching Sheet with Thermal Radiation. J. Thermodyn. 2013, 2013, 169674.

[5] Vijaya, K.; Reddy, G. V. R. Magneto Hydrodynamic Casson Fluid Flow Over a Vertical Porous Plate in the Presence of Radiation, Soret and Chemical Reaction Effects. J. Nanofluids 2019, 8, 1240–1248.

Received: July 14, 2025

Volume 38 No. 1s, 2025

ISSN: 1311-1728 (printed version); ISSN: 1314-8060 (on-line version)

[6] Santoshi, P. N.; Reddy, G. V. R.; Reddy, M. G.; Padma, P. Heat and Mass Transfer of Non-Newtonian Nano fluid Flow Over a Stretching Sheet with Non-Uniform Heat Source and Variable Viscosity. J. Nanofluids 2018, 7, 821–832.

[7] Kallepalli, N. S.; Rajasekhar, K.; Ramana, C. V. Influence of Critical Parameters on an Unsteady State MHD Flow in a Porous Channel with Exponentially Decreasing Suction. J. Math. Comput. Sci. 2019, 9, 764–783.

[8] Sivaiah, G.; Reddy, K. J.; Reddy, P. C.; Raju, M. C. Numerical Study of MHD Boundary Layer Flow of a Viscoelastic and Dissipative Fluid Past a Porous Plate Journal of Computational Biophysics and Chemistry the Presence of Thermal Radiation. Int. J. Fluid Mech. Res. 2019, 46,27–38.

[9] Reddy, G. V. R.; Krishna, Y. H. Soret and Dufour Effects on MHD Micropolar Fluid Flow Over a Linearly Stretching Sheet, Through a Non-Darcy Porous Medi um. Int. J. Appl. Mech. Eng. 2018, 23, 485–502.

[10] Sujatha, T.; Reddy, K. J.; Kumar, J. G. Chemical Reac tion Effect on Nonlinear Radiative MHD Nanofluid Flow Over Cone and Wedge. Defect Diffus. 2019, 393, 83–102

[11] Ibrahim, S. M.; Mabood, F.; Suneetha, K.; Lorenzini, G. Effects of Chemical Reaction on Combined Heat and Mass Transfer by Laminar Mixed Convection Flow from Vertical Surface with Induced Magnetic Field and Radiation. J. Eng. Thermophys. 2017, 26, 234–255.

[12] Kumar, G. C.; Reddy, K. J.; Ramakrishna, K.; Reddy, M. N. Non-Uniform Heat Source/Sink and Joule Heating Effects on Chemically Radiative MHD Mixed Convective Flow of Micropolar Fluid Over a Stretching Sheet in Porous Medium. Defect Diffus. 2018, 388, 281 302.

[13] Padmavathi, T.; Senthamilselvi, S.; Karuppusamy, L.; Oluwole, D. M.; Sarris, I. E. Mass Transfer Effects on the Mucus Fluid with Pulsatile Flow Influence of the Elec tromagnetic Field Inventions 2022, 7, 50.

[14] Abbas Yusuf Balarabe, Yale Ibrahim Danjumma, Gado Abubakar Abubakar, Yakubu Ibrahim Barga. Unsteady MHD flow of heat and mass transfer for second grade fluid in the presence of thermal radiation. International Journal of Multidisciplinary Research and Growth Evaluation.Vol-4, 122-128 2582-7138.

[15] Farhan Ai, Zaib. A, Khalid. M Unsteady MHD Flow of casson fluid past Vertical Surface Using Laplace Transform Solution. Journal of Computational Biophysics and Chemistry, 2023, 22(3), 361-370.

Received: July 14, 2025